Inorg. Chem. **2002**, *41*, 4158–4166

Mechanistic Studies on the Reactions of PhS^- or $[MoS_4]^{2-}$ with $[M_4(SPh)_{10}]^{2-}$ (M = Fe or Co)

Zhen Cui[†] **and Richard A Henderson***[,‡]

Department of Biological Chemistry, John Innes Centre, Colney, Norwich NR4 7UH, U.K., and Department of Chemistry, Bedson Building, University of Newcastle, Newcastle-upon-Tyne NE1 7RU, U.K.

Received April 18, 2002

Kinetic studies, using stopped-flow spectrophotometry, on the reactions of $[M_4(SPh)_{10}]^{2-}$ (M = Fe or Co) with PhS^- to form $[M(SPh)_4]^{2-}$ are described, as are the reactions between $[M_4(SPh)_{10}]^{2-}$ and $[MoS_4]^{2-}$ to form $[S_2MoS_2Fe(SPh)_2]^{2-}$ or $[S_2MoS_2CoS_2MoS_2]^{2-}$. The kinetics of the reactions with PhS^- are consistent with an initial associative substitution mechanism involving attack of PhS^- at one of the tetrahedral M sites of $[M_4(SPh)_{10}]^{2-}$ to form $[M_4(SPh)_{11}]^{3-}$. Subsequent or concomitant cleavage of a μ-SPh ligand, at the same M, initiates a cascade of rapid reactions which result ultimately in the complete rupture of the cluster and formation of $[M(SPh)_4]^{2-}$. The kinetics of the reaction between $[M_4(SPh)_{10}]^{2-}$ and $[MoS_4]^{2-}$ indicate an initial dissociative substitution mechanism at low concentrations of $[MoS_4]^{2-}$, in which rate-limiting dissociation of a terminal thiolate from $[M_4(SPh)_{10}]^{2-}$ produces $[M_4(SPh)_9]^-$ and the coordinatively unsaturated M site is rapidly attacked by a sulfido group of $[MoS_4]^{2-}$. It is proposed that subsequent chelation of the MoS_4 ligand results in cleavage of an M-μ-SPh bond, initiating a cascade of reactions which lead to the ultimate break-up of the cluster and formation of the products, $[S_2MoS_2Fe(SPh)_2]^{2-}$ or $[S_2MoS_2CoS_2MoS_2]^{2-}$. With $[Co_4(SPh)_{10}]^{2-}$, at higher concentrations of $[MoS_4]^{2-}$, a further substitution pathway is evident which exhibits a second order dependence on the concentration of $[MoS_4]^{2-}$. The mechanistic picture of cluster disruption which emerges from these studies rationalizes the "all or nothing" reactivity of $[M_4(SPh)_{10}]^{2-}$.

Introduction

The mechanisms of substitution reactions of transition metal complexes are now well-defined for a variety of different geometries, including metal clusters.[1] One particular area that we have focused on is the substitution mechanisms of synthetic[2,3] and natural[4] Fe−S-based clusters, where both dissociative and associative mechanisms can operate. For simplicity, work to date on Fe−S-based clusters has been restricted to studies where the integrity of the cluster core framework is maintained. Indeed, in general, there have been few mechanistic studies on reactions in which the cluster core changes. However, understanding the mechanisms of reactions where there is an increase or decrease in the nuclearity of clusters is fundamental to the future design and rational synthesis of new clusters, as well as the definition of the chemical basis of cluster biosynthesis. In this paper, we report kinetic studies on the reactions of $[M_4(SPh)_{10}]^{2-}$ (M = Fe or Co) in which initial substitution at one metal site leads ultimately to the rupture of the entire cluster and formation of products containing only a single M center.

Clusters of the type $[M_4(SPh)_{10}]^{2-}$ (M = Fe, Co and Zn) have an "adamantane-like" structure in which each M is tetrahedral and contains one terminal thiolate and three thiolates bridging to the other metals.[5−7] It has been shown that $[Fe_4(SPh)_{10}]^{2-}$ is an important species in the formation of cuboidal Fe−S-based clusters.[5] Thus, in acetonitrile, $[Fe_4(SPh)_{10}]^{2-}$ is the first identifiable species formed in the reaction between $FeCl_2$ and limiting amounts of NaSPh. Addition of elemental sulfur to $[Fe_4(SPh)_{10}]^{2-}$ results in the

* To whom correspondence should be addressed. E-mail: r.a.henderson@ncl.ac.uk.
[†] John Innes Centre.
[‡] University of Newcastle.

(1) Tobe, M. L.; Burgess, J. *Inorganic Reaction Mechanisms*; Longman: Harlow, U.K., 1999 and refs therein.
(2) Henderson, R. A. *J. Chem. Soc., Dalton Trans*. **1999**, 119.
(3) Gronberg, K. L. C.; Henderson, R. A.; Oglieve, K. E. *J. Chem. Soc., Dalton Trans*. **1997**, 1507.
(4) Gronberg, K. L. C.; Gormal, C. A.; Durrant, M. C.; Smith, B. E.; Henderson, R. A. *J. Am. Chem. Soc*. **1998**, *120*, 10613.
(5) Hagen, K. S.; Reynolds, J. G.; Holm, R. H. *J. Am. Chem. Soc*. **1981**, *103*, 4054.
(6) Dance, I. G. *J. Am. Chem. Soc*. **1979**, *101*, 6264.
(7) Dance, I. G. *J. Am. Chem. Soc*. **1980**, *102*, 3445.

10.1021/ic020284j CCC: $22.00
Published on Web 07/11/2002

ultimate formation of $[Fe_4S_4(SPh)_4]^{2-}$, while addition of $[M'S_4]^{2-}$ (M′ = Mo, W, or V)[8–10] ultimately produces the dicubane clusters, $[\{M'Fe_3S_4(SPh)_3\}_2(\mu\text{-}SPh)_3]^{3-}$.

Herein, we report kinetic studies on the rapid reactions of $[M_4(SPh)_{10}]^{2-}$ (M = Fe and Co) with an excess of PhS^- to produce $[M(SPh)_4]^{2-}$ as described by eq 1, and with $[MoS_4]^{2-}$ to form $[S_2MoS_2Fe(SPh)_2]^{2-}$ or $[S_2MoS_2CoS_2MoS_2]^{2-}$ as described by eqs 2 and 3, respectively.

$$[M_4(SPh)_{10}]^{2-} + 6PhS^- \rightarrow 4[M(SPh)_4]^{2-} \quad (1)$$

$$[Fe_4(SPh)_{10}]^{2-} + 4[MoS_4]^{2-} \rightarrow 4[S_2MoS_2Fe(SPh)_2]^{2-} + 2PhS^- \quad (2)$$

$$[Co_4(SPh)_{10}]^{2-} + 8[MoS_4]^{2-} \rightarrow 4[S_2MoS_2CoS_2MoS_2]^{2-} + 10PhS^- \quad (3)$$

All these reactions are clearly multistep processes and involve the disruption of the entire cluster framework. Furthermore, eqs 2 and 3 are idealized stoichiometries because any free PhS^- in solution can compete with $[MoS_4]^{2-}$ in reacting with $[M_4(SPh)_{10}]^{2-}$ to produce some $[M(SPh)_4]^{2-}$, according to eq 1. As indicated previously, the reaction shown in eq 2 is the initial stage in the formation of the cuboidal cluster, $[\{MoFe_3S_4(SPh)_3\}_2(\mu\text{-}SPh)_3]^{3-}$. However, the reaction in eq 2 is appreciably faster than the cuboidal cluster formation and hence is easily studied without any complications arising from further reactions.

Experimental Section

All manipulations in the preparation of the compounds were routinely performed under an atmosphere of dinitrogen using Schlenk and syringe techniques as appropriate. Because of the extreme air-sensitivity of the dilute solutions of $[NMe_4]_2[Co_4(SPh)_{10}]$ used in the ^1H NMR spectroscopic and kinetic experiments, samples were prepared in a Saffron glovebox operating at less than 1 ppm dioxygen. All solvents were dried and distilled under dinitrogen immediately prior to use.

The clusters $[NEt_4]_2[Fe_4(SPh)_{10}]$[5] and $[NMe_4]_2[Co_4(SPh)_{10}]$[6] were prepared by the literature methods and characterized by elemental analysis and comparison of the ^1H NMR spectrum with that reported in the literature. $[NEt_4]SPh$,[11] $[NHEt_3]BPh_4$,[12] $[NEt_4]_2[MS_4]$ (M = Mo or W),[13] and $[NEt_4]_3[VS_4]$[14] were prepared by methods reported in the literature.

The ^1H NMR spectrum of $[NMe_4]_2[Co_4(SPh)_{10}]$, which has not been reported before, is shown in Figure 1. All ^1H NMR spectra were recorded on a JEOL Lambda 400 instrument. The peaks in the spectrum of $[Co_4(SPh)_{10}]^{2-}$ were assigned using the following criteria: (i) the relative intensities, (ii) that *o*-H atoms will be broader than *m*- or *p*-H because of the proximity to the paramagnetic cobalt atoms, and (iii) the comparison with the spectrum of $[Fe_4(SPh)_{10}]^{2-}$, δ 13.0 (*m*-H_t); 11.6 (*m*-H_b); −11.8 (*p*-H_t); −14.8 (*p*-H_b); −16.2 (*o*-H_t); −24.1 (*o*-H_b). The subscripts b and t designate bridging and terminal ligands, respectively. Elemental Anal. $[NMe_4]_2[Co_4(SPh)_{10}]$ Calcd: C, 55.4; H, 5.0; N, 1.9; S, 21.7%. Found: C, 55.2; H, 4.9; N, 1.8; S, 19.7%.

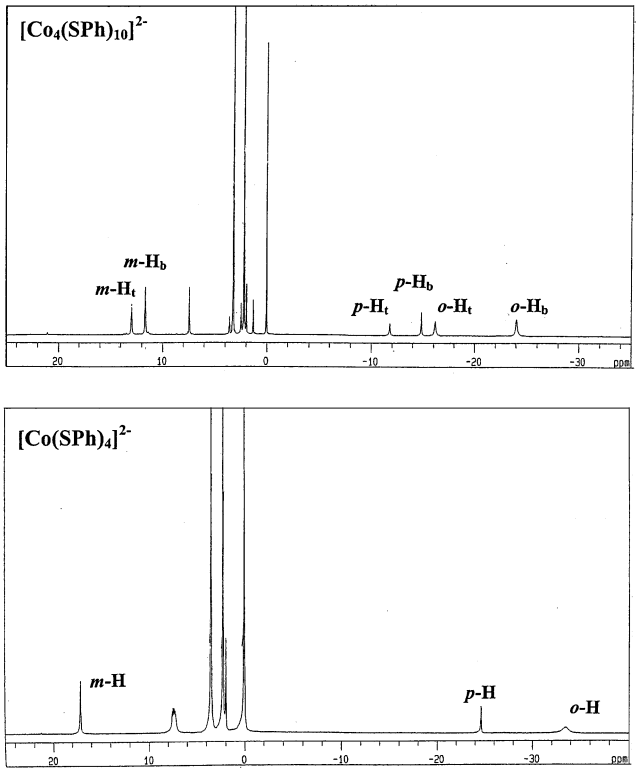

Figure 1. ^1H NMR spectra of $[NMe_4]_2[Co_4(SPh)_{10}]$ (top) and $[NMe_4]_2[Co(SPh)_4]$ (bottom), recorded in CD_3CN.

Kinetic Studies. The kinetics of the reactions between the cluster $[M_4(SPh)_{10}]^{2-}$ (M = Fe or Co) and PhS^- or $[MoS_4]^{2-}$ were studied in MeCN using a Hi-Tech SF-51 stopped-flow spectrophotometer, modified to handle air-sensitive solutions.[15] The temperature was maintained at 25.0 °C using a Grant LE8 thermostat tank. The spectrophotometer was interfaced to a computer via an analogue-to-digital converter. All data collected were transferred directly to the computer and analyzed using a curve-fitting program.

Solutions of $[NEt_4]SPh$ and $[NEt_4]_2[MoS_4]$ were prepared from stock solutions of the reagents and used within 1 h of preparation. All reactions were carried out under pseudo-first-order conditions, with an excess of nucleophile, PhS^- and $[MoS_4]^{2-}$, such that [nucleophile]/$[M_4(SPh)_{10}{}^{2-}] \geq 20$. The kinetics of the reactions of $[Fe_4(SPh)_{10}]^{2-}$ were monitored by following the absorbance change at λ = 550 or 600 nm as indicated in the legends of the figures. The absorbance−time traces were fitted to a single exponential curve using a computer program, and the values of the observed rate constants (k_{obs}) were obtained from the computer analysis. The dependences on the concentrations of nucleophiles were established by the usual graphical procedures,[16] as indicated for each case in the Results section.

Identification of Products. The product of the reaction between $[Fe_4(SPh)_{10}]^{2-}$ and an excess of PhS^- was identified as $[Fe(SPh)_4]^{2-}$

(8) Wolff, T. E.; Power, P. P.; Frankel, R. B.; Holm, R. H. *J. Am. Chem. Soc.* **1980**, *102*, 4694.
(9) Henderson, R. A.; Oglieve, K. E. *J. Chem. Soc., Dalton Trans.* **1993**, 1473.
(10) Cen, W.; Lee, S. C.; Li, J.; MacDonnell, F. M.; Holm, R. H. *J. Am. Chem. Soc.* **1993**, *115*, 9515.
(11) Palermo, R. E.; Power, P. P.; Holm, R. H. *Inorg. Chem.* **1982**, *21*, 173.
(12) Dilworth, J. R.; Henderson, R. A.; Dahlstrom, P.; Nicholson, T.; Zubieta, J. A. *J. Chem. Soc., Dalton Trans.* **1987**, 529.
(13) Diemann, E.; Müller, A. *Coord. Chem. Rev.* **1973**, *10*, 79.
(14) Do, V.; Simhon, E. D.; Holm, R. H. *Inorg. Chem.* **1985**, *24*, 4635.
(15) Henderson, R. A. *J. Chem. Soc., Dalton Trans.* **1982**, 917.
(16) Wilkins, R. G. *Kinetics and Mechanism of Reactions of Transition Metal Complexes*; VCH: Weinheim, 1991.

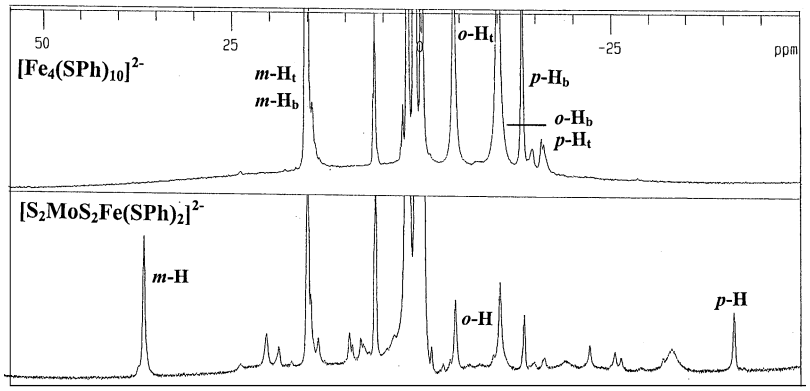

Figure 2. ^{1}H NMR spectra in CD_3CN of $[Fe_4(SPh)_{10}]^{2-}$ (top) and the reaction product of $[Fe_4(SPh)_{10}]^{2-}$ with 3.5 mol equiv of $[MoS_4]^{2-}$ (ca. 5 min after mixing) to produce $[S_2MoS_2Fe(SPh)_2]^{2-}$ (bottom). Apart from the resonances attributable to $[S_2MoS_2Fe(SPh)_2]^{2-}$ and residual $[Fe_4(SPh)_{10}]^{2-}$, peaks due to $[Fe(SPh)_4]^{2-}$ are also evident (see Experimental Section). Both spectra were recorded with the same attenuation.

by ^{1}H NMR spectroscopy with paramagnetic shifts of δ 22.8 (*m*-H), −16.6 (*o*-H), and −24.2 (*p*-H) ppm and comparison with the literature spectra:[5] 22.3 (*m*-H), −16.8 (*o*-H), and −23.5 (*p*-H) ppm.

The product of the reaction between $[Co_4(SPh)_{10}]^{2-}$ and an excess of PhS^- was identified as $[Co(SPh)_4]^{2-}$ by comparison with the ^{1}H NMR spectra of an authentic sample[17] of $[NMe_4]_2[Co(SPh)_4]$. The spectrum is shown in Figure 1, and the assignments were made by comparison with those of $[Fe(SPh)_4]^{2-}$: δ 17.1 (*m*-H), −33.4 (*o*-H), and −24.6 (*p*-H) ppm.

The product of the reaction between $[Fe_4(SPh)_{10}]^{2-}$ and $[MoS_4]^{2-}$ was established as $[S_2MoS_2Fe(SPh)_2]^{2-}$ using ^{1}H NMR spectroscopy as shown in Figure 2. The identity of the product was established by its characteristic peaks in the ^{1}H NMR spectrum at δ −7.0 (*o*-H), −40.0 (*p*-H), and 37.0 (*m*-H), at 25.0 °C, and comparison with the values reported in the literature:[18] δ −7.2 (*o*-H), −40.2 (*p*-H) and 39.4 (*m*-H).

The product of the reaction between $[NMe_4]_2[Co_4(SPh)_{10}]$ and $[NMe_4]_2[MoS_4]$ was tentatively identified as $[NMe_4]_2[S_2MoS_2CoS_2MoS_2]$. This cluster has not been reported before, but the analogous $[S_2WS_2CoS_2WS_2]^{2-}$ has previously been reported and characterized.[19]

A solution of $[NMe_4]_2[Co_4(SPh)_{10}]$ (1.2 g; 0.8 mmol) and $[NMe_4]_2[MoS_4]$ (1.66 g; 4.4 mmol) was stirred in MeCN (ca. 20 mL). After ca. 1 h, the solution was bright green, and a black solid had been deposited. The solid was removed by filtration, washed with cold MeCN, followed by diethyl ether, and then dried in vacuo. Elemental analysis indicated the solid was $[NMe_4]_2[S_2MoS_2CoS_2MoS_2]$. Anal. Calcd: C, 14.7; H, 3.7; N, 4.3; Co, 9.0; Mo, 29.3%. Found: C, 15.3; H, 3.7; N, 5.2; Co, 9.4%. We have been unable to obtain reproducible S or Mo analyses for this material. The ^{1}H NMR spectrum of the solid was recorded (in d^6-dmso) but showed no peaks other than the singlet due to the N−CH_3 groups of the cation. The ^{1}H NMR spectrum of the green filtrate showed that the only identifiable species present were PhS^- and $[Co(SPh)_4]^{2-}$.

Results

Reactions of $[M_4(SPh)_{10}]^{2-}$ with PhS^-. The reactions of both $[Fe_4(SPh)_{10}]^{2-}$ and $[Co_4(SPh)_{10}]^{2-}$ with an excess of PhS^- in MeCN produce the corresponding $[M(SPh)_4]^{2-}$, according to the stoichiometry shown in eq 1. When studied using stopped-flow spectrophotometry, the reactions between $[M_4(SPh)_{10}]^{2-}$ (0.20 mmol dm^{-3}) and an excess of PhS^- exhibit a first order dependence on the concentrations of both cluster and PhS^-, as defined by eq 4 and illustrated in Figure 3, with $k_1^{Fe} = 2.5 \pm 0.3 \times 10^2$ dm^3 mol^{-1} s^{-1} and $k_1^{Co} = 6.5 \pm 0.3 \times 10^2$ dm^3 mol^{-1} s^{-1}.

$$\frac{-\mathrm{d}[M_4(SPh)_{10}{}^{2-}]}{\mathrm{d}t} = k_1{}^{M}[M_4(SPh)_{10}{}^{2-}][PhS^-] \qquad (4)$$

Reactions of $[M_4(SPh)_{10}]^{2-}$ with $[MoS_4]^{2-}$. The reaction of $[Fe_4(SPh)_{10}]^{2-}$ with $[MoS_4]^{2-}$ in MeCN is described by eq 2. The kinetics of the reaction between $[Fe_4(SPh)_{10}]^{2-}$ and an excess of $[MoS_4]^{2-}$ in MeCN exhibit a first order dependence on the concentration of cluster but are independent of the concentration of $[MoS_4]^{2-}$ [Figure 4 (inset)], with $k_3^{Fe} = 1.7 \pm 0.3$ s^{-1}. The analogous reactions between $[Fe_4(SPh)_{10}]^{2-}$ and $[WS_4]^{2-}$ (to form $[S_2WS_2Fe(SPh)_2]^{2-}$) or $[VS_4]^{3-}$ (to form $[(PhS)_2FeS_2VS_2Fe(SPh)_2]^{3-}$) have also been studied, and the rates are identical to that observed with $[MoS_4]^{2-}$ ($k = 1.8 \pm 0.4$ s^{-1}).

To gain further insight into the mechanism of the reaction between $[Fe_4(SPh)_{10}]^{2-}$ and $[MoS_4]^{2-}$, the effect of adding PhS^- was investigated. The results are shown in Figure 4. Clearly, the behavior is complicated. At low concentrations of PhS^-, the reaction between $[MoS_4]^{2-}$ and $[Fe_4(SPh)_{10}]^{2-}$ is inhibited. However, as the concentration of PhS^- is increased, k_{obs} reaches a minimum and then increases linearly with the concentration of PhS^-. To interpret this behavior, we need also to consider the kinetics of the reaction between $[Fe_4(SPh)_{10}]^{2-}$ and PhS^- as described by eq 4, M = Fe. The effect of PhS^- on the reaction between $[Fe_4(SPh)_{10}]^{2-}$ and $[MoS_4]^{2-}$ can be fitted to the expression shown in eq 5. At low concentrations of PhS^-, the dominant (faster) reaction is that between $[Fe_4(SPh)_{10}]^{2-}$ and $[MoS_4]^{2-}$ to form $[S_2MoS_2Fe(SPh)_2]^{2-}$. This reaction is inhibited by PhS^-, and it corresponds to the first term of eq 5. At high concentrations of PhS^-, the dominant reaction becomes the reaction between $[Fe_4(SPh)_{10}]^{2-}$ and PhS^- to form $[Fe(SPh)_4]^{2-}$. The formation of $[Fe(SPh)_4]^{2-}$ is represented by the second term in eq 5,

(17) Hollebone, B. R.; Nyholm, R. S. *J. Chem. Soc. A* **1971**, 332.
(18) Tieckelmann, R. H.; Silvis, H. C.; Kent, T. A.; Huynh, B. H.; Waszczak, J. V.; Teo, B. K.; Averill, B. A. *J. Am. Chem. Soc.* **1980**, *102*, 5550.
(19) Müller, A.; Ahlborn, E.; Heinsen, H. H. *Z. Anorg. Allg. Chem.* **1971**, *386*, 102.

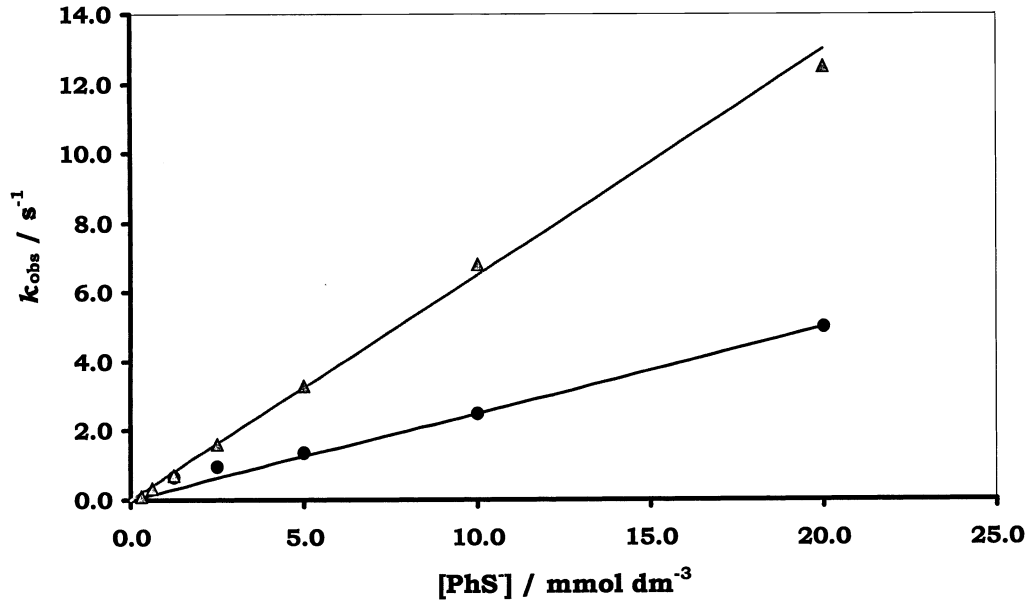

Figure 3. Kinetics of the reaction between $[M_4(SPh)_{10}]^{2-}$ [M = Fe (●) or Co (▲); 0.1 mmol dm^{-3}] and PhS^- in MeCN at 25.0 °C (λ = 550 nm).

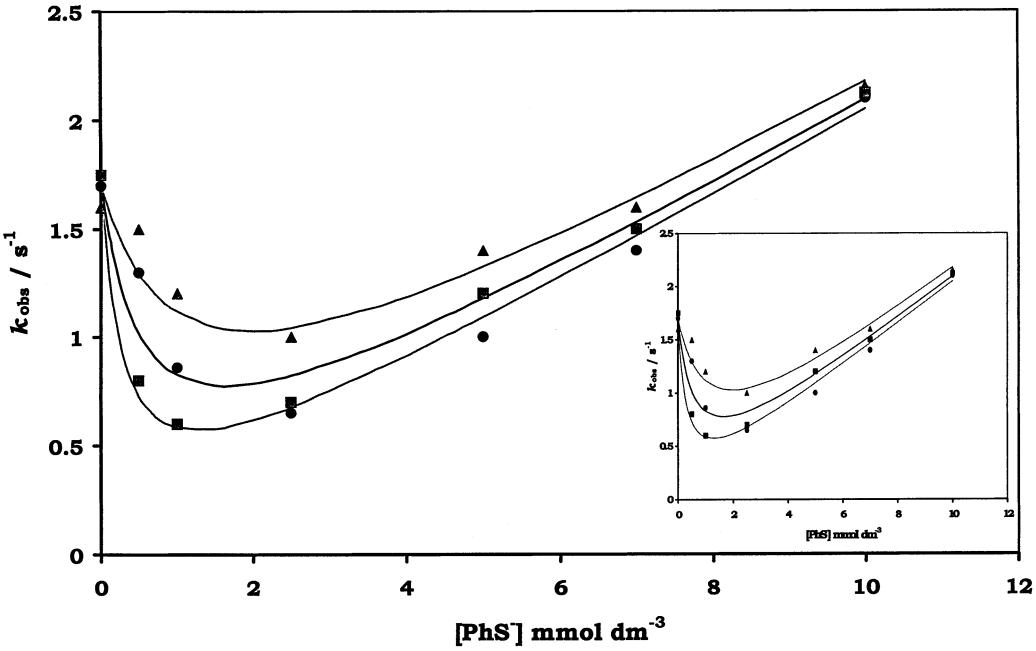

Figure 4. Kinetics of the reaction between $[Fe_4(SPh)_{10}]^{2-}$ (0.1 mmol dm^{-3}) and $[MoS_4]^{2-}$ in the presence of an excess of PhS^-, measured at λ = 600 nm in MeCN at 25.0 °C. Data points correspond to $[MoS_4^{2-}]$ = 0.025 mmol dm^{-3} (■); $[MoS_4^{2-}]$ = 0.05 mmol dm^{-3} (●); $[MoS_4^{2-}]$ = 0.10 mmol dm^{-3} (▲). Curve drawn is that defined by eq 5. Inset: Kinetics of the reaction between $[Fe_4(SPh)_{10}]^{2-}$ (0.05 mmol dm^{-3}) and $[MoS_4]^{2-}$ (●), $[WS_4]^{2-}$ (■), or $[VS_4]^{3-}$ (▲) in MeCN at 25.0 °C.

and the derived rate constant is in good agreement with the rate constant determined in the kinetic studies on the reaction between $[Fe_4(SPh)_{10}]^{2-}$ and PhS^- ($k_1^{Fe} = 2.5 \pm 0.3 \times 10^2$ dm^3 mol^{-1} s^{-1}), described previously.

$$\frac{-d[Fe_4(SPh)_{10}{}^{2-}]}{dt} = \left\{\frac{1.7 \pm 0.3}{1 + 0.09 \pm 0.01[PhS^-]/[MoS_4{}^{2-}]} + 2.0 \pm 0.2 \times 10^2[PhS^-]\right\}[Fe_4(SPh)_{10}{}^{2-}] \quad (5)$$

Consistent with the previously described interpretation of the kinetics, ^1H NMR spectroscopic studies show that the reaction between solutions of $[Fe_4(SPh)_{10}]^{2-}$ (0.5 mmol dm^{-3}) and $[MoS_4]^{2-}$ (2.0 mmol dm^{-3}) in MeCN produces $[S_2MoS_2Fe(SPh)_2]^{2-}$, with only a trace of $[Fe(SPh)_4]^{2-}$. However, under analogous conditions, the reaction between $[Fe_4(SPh)_{10}]^{2-}$ (0.5 mmol dm^{-3}) and $[MoS_4]^{2-}$ (2.0 mmol dm^{-3}) in the presence of PhS^- (10.0 mmol dm^{-3}) produced exclusively $[Fe(SPh)_4]^{2-}$.

We have also studied the effect of PhS^- on the reaction between $[Fe_4(SPh)_{10}]^{2-}$ and $[WS_4]^{2-}$. Identical behavior to that described for the reaction of $[MoS_4]^{2-}$ is observed. At constant concentration of $[WS_4]^{2-}$, the rate constants observed in the presence of PhS^- were indistinguishable from

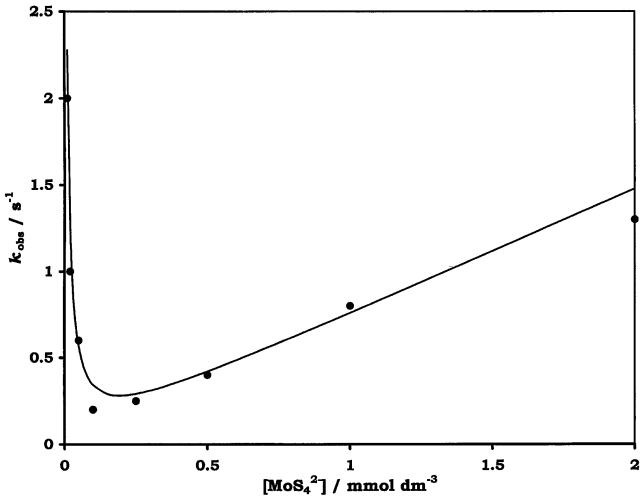

Figure 5. Kinetics of the reaction between $[Co_4(SPh)_{10}]^{2-}$ (0.05 mmol dm^{-3}) and $[MoS_4]^{2-}$ in MeCN at 25.0 °C. Curve drawn is defined by eq 6.

those in the presence of $[MoS_4]^{2-}$ (see Table 2 in the Supporting Information).

The reaction between $[Co_4(SPh)_{10}]^{2-}$ and $[MoS_4]^{2-}$ in MeCN gives $[S_2MoS_2CoS_2MoS_2]^{2-}$, as shown in eq 3. The kinetics of this reaction exhibit a first order dependence on the concentration of cluster but a complicated dependence on the concentration of $[MoS_4]^{2-}$ as shown in Figure 5 and described by eq 6.

$$\frac{-\mathrm{d}[Co_4(SPh)_{10}{}^{2-}]}{\mathrm{d}t} = \frac{\{12.5 \pm 1.0 + 3.3 \pm 0.2 \times 10^8[MoS_4{}^{2-}]^2\}[Co_4(SPh)_{10}{}^{2-}]}{1 + 4.5 \pm 0.5 \times 10^5[MoS_4{}^{2-}]} \quad (6)$$

In the presence of PhS^-, the reaction between $[Co_4(SPh)_{10}]^{2-}$ and $[MoS_4]^{2-}$ is associated with simple kinetics, in which the rate exhibits a first order dependence on the concentration of cluster and PhS^- but is independent of the concentration of $[MoS_4]^{2-}$ ($k = 6.5 \pm 0.3 \times 10^2$ dm^3 mol^{-1} s^{-1}). These kinetics are identical to those for the reaction between $[Co_4(SPh)_{10}]^{2-}$ and PhS^- as described by eq 4, M = Co. The kinetics thus correspond to the formation of $[Co(SPh)_4]^{2-}$. Under the conditions used, $[Co_4(SPh)_{10}]^{2-}$ reacts faster with PhS^- than with $[MoS_4]^{2-}$. Similar behavior was observed in the analogous reaction of $[Fe_4(SPh)_{10}]^{2-}$ with $[MoS_4]^{2-}$ in the presence of PhS^-. However, in the Fe system, the rate of formation of $[Fe(SPh)_4]^{2-}$ only becomes faster than the reaction between $[Fe_4(SPh)_{10}]^{2-}$ and $[MoS_4]^{2-}$ at high concentrations of PhS^- (Figure 4).

Discussion

Associative Mechanism. The kinetics of the reactions of $[M_4(SPh)_{10}]^{2-}$ with PhS^- (eq 4) are consistent with the associative mechanism shown in Figure 6. A persistent feature of this mechanism (and others that follow in this paper) is the maintenance of four-coordination at each metal site throughout the transformation. Thus, attack of PhS^- at a metal site is accompanied by cleavage of a bridging thiolate. It is this initial step which starts a cascade of rapid reactions which result ultimately in the complete rupture of the cluster and stoichiometric formation of $[M(SPh)_4]^{2-}$.

The kinetics in eq 4 are consistent with the initial steps in the reaction between $[M_4(SPh)_{10}]^{2-}$ and PhS^- being those shown in Figure 6. Either attack of PhS^- on $[M_4(SPh)_{10}]^{2-}$ is rate-limiting (in which case, $k_{obs} = k_1\mathrm{M}[PhS^-]$), or dissociation of the μ-SPh after, or concomitant with, attack by free PhS^- is rate-limiting {in which case, $k_{obs} = k_1{}^{\mathrm{M}}k_2{}^{\mathrm{M}}[PhS^-]/(k_{-1}{}^{\mathrm{M}} + k_2{}^{\mathrm{M}})$}.

There are two indications that after the initial attack of PhS^- the subsequent reactions of $[M_4(SPh)_{11}]^{3-}$ must be fast. First, the stopped-flow traces can be fitted to a single exponential with an initial absorbance corresponding to $[M_4(SPh)_{10}]^{2-}$ and a final absorbance to $[M(SPh)_4]^{2-}$. Second, "all or nothing" reactivity is exhibited by these clusters (vide infra).

Although the kinetics only reveal information about the initial reaction of $[M_4(SPh)_{10}]^{2-}$, we propose here a mechanism for the complete rupture of the cluster. It seems unlikely that the cleavage of a single μ-PhS ligand is sufficient to result in the immediate rupture of the entire cluster. If we consider the structural changes to the cluster, it is evident that, whereas in $[M_4(SPh)_{10}]^{2-}$ all M sites are equivalent, $[M_4(SPh)_{11}]^{3-}$ has a more open structure with two distinct types of metal sites (Figure 6). Two of the sites (M_a) are identical to those in the parent cluster (with one terminal and three bridging thiolate ligands), whereas the other two sites (M_b) contain two terminal and two bridging thiolate ligands. The rational and systematic mechanism for cluster rupture we propose (Figure 7) requires that cleavage of a M_a-μ-SPh bond (where the thiolate is bridging between a M_a and M_b site) occurs in $[M_4(SPh)_{11}]^{3-}$. This cleavage naturally generates a vacant site on M_a, thus facilitating attack of another PhS^-. The sequence of reactions shown in Figure 7 involves repetition of the elementary steps observed in the initial stage: cleavage of a μ-SPh and binding of free PhS^- to the metal site from which the μ-SPh has dissociated.

Dissociative Mechanism. In the reaction between $[M_4(SPh)_{10}]^{2-}$ and an excess of $[MoS_4]^{2-}$, the kinetics observed at low concentrations of $[MoS_4]^{2-}$ are consistent with an initial dissociative substitution mechanism as shown at the beginning of Figure 8. Initial rate-limiting dissociation of a terminal thiolate ligand from $[M_4(SPh)_{10}]^{2-}$ generates $[M_4(SPh)_9]^-$, and rapid attack of a sulfido ligand of $[MoS_4]^{2-}$ at the vacant site generates $[M_4(SPh)_9(SMoS_3)]^{3-}$. It seems unlikely that merely binding $[MoS_4]^{2-}$ to one metal site is sufficiently labilizing to result in the entire rupture of the cluster. Indeed, we have already discussed that in the reaction of $[M_4(SPh)_{10}]^{2-}$ with PhS^- it is the associative attack of PhS^- at one M, and the concomitant cleavage of a μ-SPh linkage, which leads to the progressive rupture of the cluster. We propose that in the reactions of $[M_4(SPh)_{10}]^{2-}$ with $[MoS_4]^{2-}$ it is chelation of the monodentate MoS_4 ligand which is the key step leading to cluster fragmentation. In order that the M sites are to remain four-coordinate, chelation

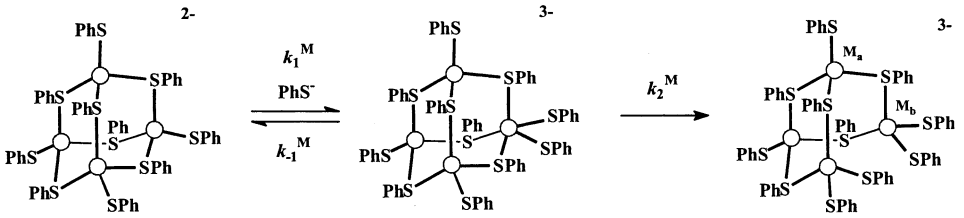

Figure 6. Details of the initiating steps in the associative mechanism of the reaction between $[M_4(SPh)_{10}]^{2-}$ (M = Fe or Co) and PhS^- in MeCN.

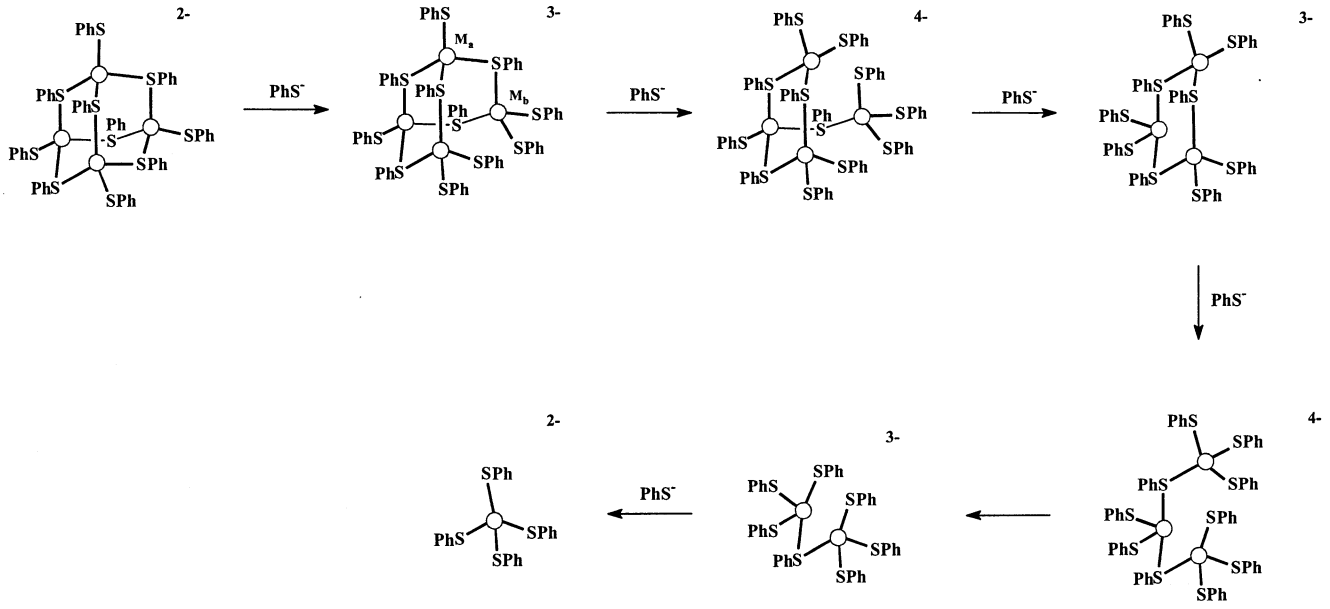

Figure 7. Associative mechanism for the reaction between $[M_4(SPh)_{10}]^{2-}$ (M = Fe or Co) and PhS^- in MeCN.

of the monodentate MoS_4 ligand in $[M_4(SPh)_9(SMoS_3)]^{3-}$ must facilitate cleavage of a μ-SPh and start the rupture of the cluster as shown in Figure 8. Effectively, this chelation is an intramolecular associative attack at the cluster.

At this stage, we should consider the structure of the cluster after the μ-SPh cleavage reaction. $[M_4(SPh)_9(SMoS_3)]^{3-}$ contains three different types of metal sites as indicated in Figure 8. Two M_a sites are unchanged from the M sites in $[M_4(SPh)_{10}]^{2-}$, one M_b site contains two terminal and two bridging thiolate ligands, and one M_c site is bound to MoS_4. We propose that the electron-withdrawing ability of the Mo^{VI} center weakens a M_a-μ-SPh bond leading to cleavage of the bond and generating a vacant site on this M_a at which $[MoS_4]^{2-}$ can attack. The progressive break-up of the cluster occurs by repetition of the following elementary steps: chelation of MoS_4 ligand and dissociation of M-μ-SPh linkage generating a new vacant site on the adjacent M at which another $[MoS_4]^{2-}$ binds.

At low concentrations of PhS^-, the reaction between $[Fe_4(SPh)_{10}]^{2-}$ and $[MoS_4]^{2-}$ is inhibited by the thiolate, confirming the dissociative mechanism for the initial reaction (Figure 4 and eq 5). The details of the initial steps of the mechanism are shown in Figure 8. Assuming that $[M_4(SPh)_9(SMoS_3)]^{3-}$ is a steady-state intermediate, the rate law for the dissociative mechanism is that shown in eq 7, and comparison with eq 5 gives $k_3^{Fe} = 1.7 \pm 0.3\ s^{-1}$ and $k_{-3}^{Fe}/k_4^{Fe} = 0.09 \pm 0.01$.

$$\frac{-d[M_4(SPh)_{10}^{2-}]}{dt} = \frac{\{k_3^M\}[M_4(SPh)_{10}^{2-}]}{1 + k_{-3}^M[PhS^-]/k_4^M[MoS_4^{2-}]} \quad (7)$$

It seems likely that the dissociative mechanism also dominates in the reaction between $[Co_4(SPh)_{10}]^{2-}$ and low concentrations of $[MoS_4]^{2-}$ ($k_3^{Co} = 12.5 \pm 1.0\ s^{-1}$), as discussed in the Results section. However, the reaction of $[Co_4(SPh)_{10}]^{2-}$ with PhS^- is faster than that with $[MoS_4]^{2-}$ at all concentrations. Consequently, the effect of PhS^- on the rate of the reaction between $[Co_4(SPh)_{10}]^{2-}$ and $[MoS_4]^{2-}$ cannot be measured.

The reaction between $[Co_4(SPh)_{10}]^{2-}$ and $[MoS_4]^{2-}$ produces the linear trinuclear cluster $[S_2MoS_2CoS_2MoS_2]^{2-}$. However, the kinetics are similar to those observed for $[Fe_4(SPh)_{10}]^{2-}$ where $[S_2MoS_2Fe(SPh)_2]^{2-}$ is the product. This indicates that the defining initial steps are similar for both clusters. Thus, we propose that the initial product of the reaction between $[Co_4(SPh)_{10}]^{2-}$ and $[MoS_4]^{2-}$ is $[S_2MoS_2Co(SPh)_2]^{2-}$, and only subsequent rapid reactions with $[MoS_4]^{2-}$ yield the trinuclear cluster.

The kinetics of the reaction between $[Co_4(SPh)_{10}]^{2-}$ and $[MoS_4]^{2-}$ (eq 6) show that at high concentrations of $[MoS_4]^{2-}$ the dissociative route is inhibited and a pathway which exhibits a second order dependence on the concentration of $[MoS_4]^{2-}$ becomes dominant. Because this pathway exhibits a second order dependence on the concentration of $[MoS_4]^{2-}$,

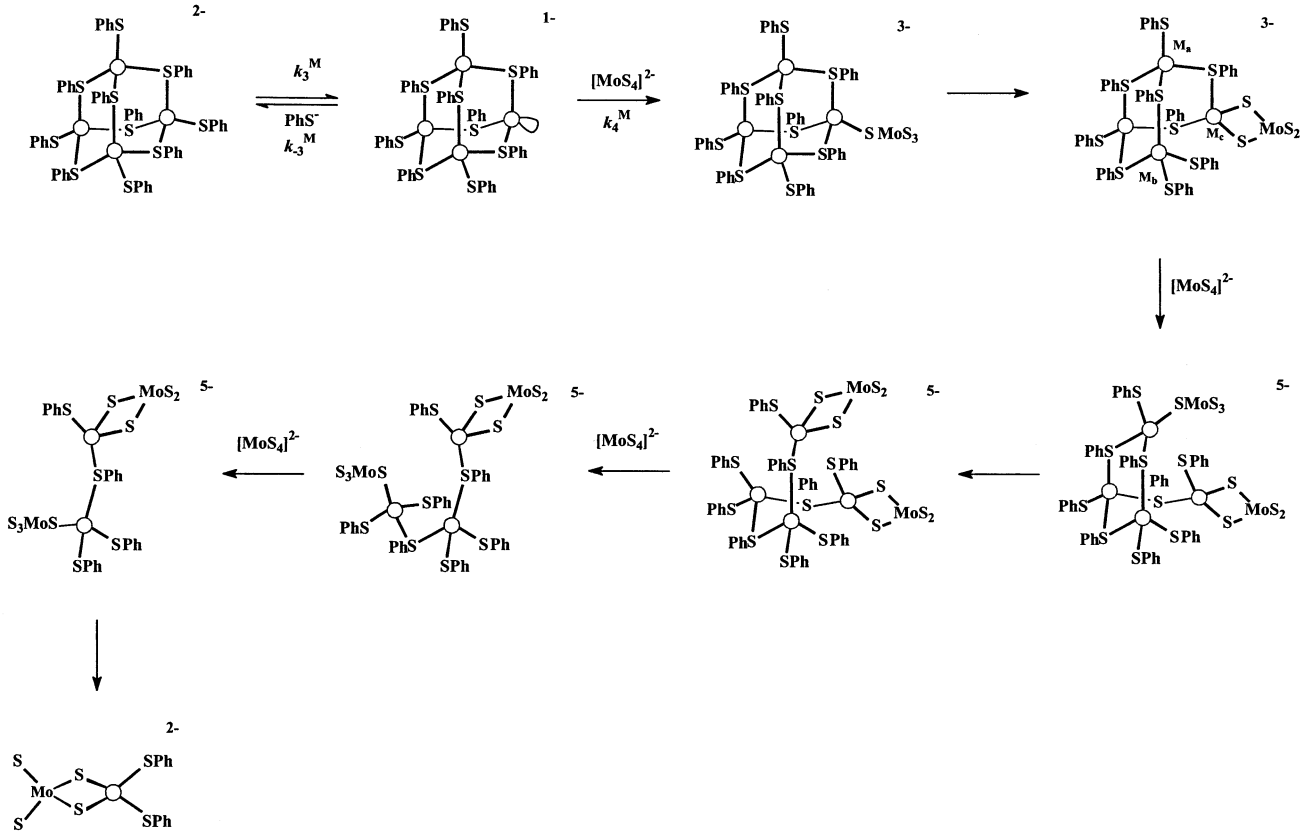

Figure 8. Dissociative mechanism for the reaction between $[M_4(SPh)_{10}]^{2-}$ (M = Fe or Co) and $[MoS_4]^{2-}$ in MeCN.

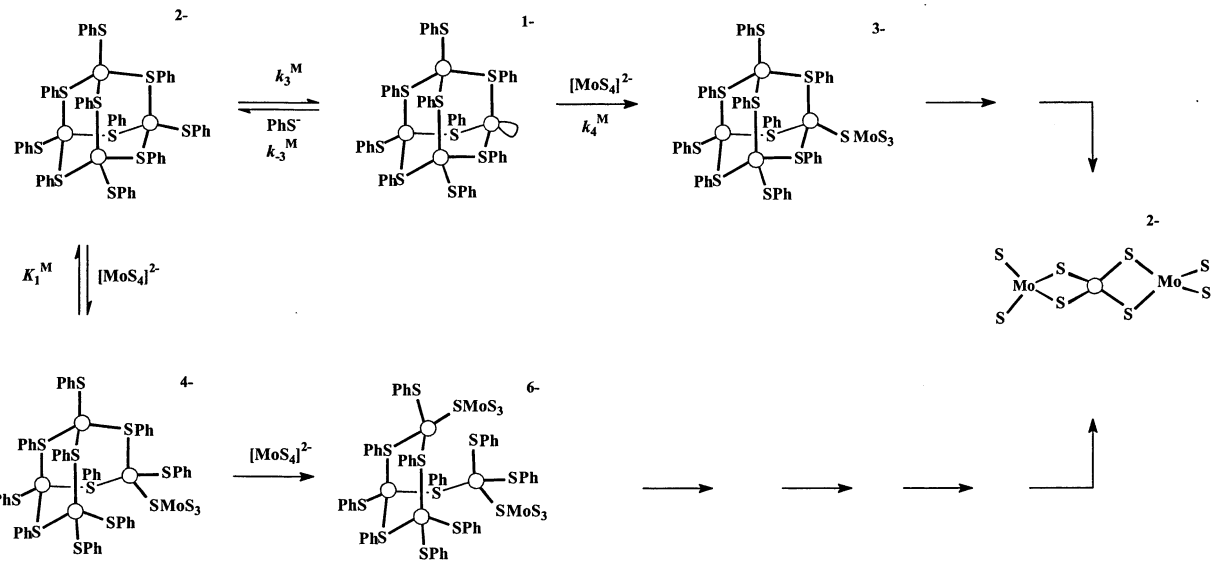

Figure 9. Details of the initiating step in the dissociative mechanism of the reaction between $[M_4(SPh)_{10}]^{2-}$ (M = Fe or Co) and $[MoS_4]^{2-}$ and the associative mechanism observed in the reaction of $[Co_4(SPh)_{10}]^{2-}$ and $[MoS_4]^{2-}$ in MeCN.

it is slower than the dissociative pathway until $[MoS_4^{2-}] > 0.25$ mmol dm^{-3}.

The second order dependence on the concentration of $[MoS_4]^{2-}$ is consistent with the pathway shown in Figure 9 in which the first $[MoS_4]^{2-}$ binds to $[Co_4(SPh)_{10}]^{2-}$ at a rate which is comparable to the initial dissociation of a terminal PhS ligand from $[Co_4(SPh)_{10}]^{2-}$. In line with the associative mechanism with PhS^- described previously, we propose that initial attack of $[MoS_4]^{2-}$ at one of the Co sites is accompanied by cleavage of a μ-SPh. The electron-withdrawing MoS_4 ligand labilizes an adjacent Co-μ-SPh bond (possibly also involving chelation of the MoS_4-ligand) and generates a vacant site on a second Co center at which the second $[MoS_4]^{2-}$ binds. A cascade of subsequent substitution reactions results in the progressive rupture of the cluster.

Consideration of the mechanism shown in the bottom line of Figure 9 gives the rate law shown in eq 8, assuming that binding of the first $[MoS_4]^{2-}$ is a rapid equilibrium reaction (K_1^{Co}). This rate law is in good agreement with that observed experimentally (eq 6), and comparison of the two equations gives $k_3^{Co} = 12.5 \pm 1.0\ s^{-1}$, $K_1^{Co} = 4.5 \pm 0.5 \times 10^5\ dm^3\ mol^{-1}$, and $k_5^{Co} = 7.4 \pm 0.5 \times 10^2\ dm^3\ mol^{-1}\ s^{-1}$.

$$\frac{-d[Co_4(SPh)_{10}^{2-}]}{dt} = \frac{\{k_3^{Co} + K_1^{Co}k_5^{Co}[MoS_4^{2-}]^2\}[Co_4(SPh)_{10}^{2-}]}{1 + K_1^{Co}[MoS_4^{2-}]} \quad (8)$$

Effect of Acid on the Reactivity of $[M_4(SPh)_{10}]^{2-}$. We have studied the effect of $[NHEt_3]^+$ on the rate of the reaction between $[Fe_4(SPh)_{10}]^{2-}$ and $[MoS_4]^{2-}$. We chose to investigate the effect of acid on this reaction because $[NHEt_3]^+$ ($pK_a = 18.4$ in MeCN)[20] is insufficiently acidic to protonate $[MoS_4]^{2-}$, and hence, any effect observed must be attributable to protonation of the cluster. Surprisingly, the rate of the reaction between $[Fe_4(SPh)_{10}]^{2-}$ and $[MoS_4]^{2-}$ is unaffected by the addition of $[NHEt_3]^+$ (see Table 3 in the Supporting Information). This is distinctly different behavior from that observed with Fe−S-based clusters.[21−25] The kinetics of the substitution of terminal ligands on Fe−S-based clusters such as $[Fe_4S_4X_4]^{2-}$, $[(MoFe_3S_4X_3)_2\{\mu\text{-SEt}\}_3]^{3-}$ (X = alkanethiolate, aryl thiolate, or halide), $[S_2MS_2Fe(SPh)_2]^{2-}$ (M = Mo or W), and $[MoFe_4S_6(PEt_3)_4Cl]$ are all catalyzed by $[NHEt_3]^+$. All synthetic Fe−S-based clusters have a pK_a in the range 17.9−18.9 in MeCN, indicating that protonation occurs at the μ_3-S atoms.[25] It seems unlikely that the μ_3-S atoms in these clusters are more basic than the sulfur atom in terminal thiolate ligands. However, if protonation at a thiolate does occur, it does not affect the rate of substitution, indicating that protonation of the cluster core (μ_3-S) is more labilizing than protonation of terminal thiolate ligands in the substitution reactions of all Fe−S-based clusters. That $[NHEt_3]^+$ does not affect the rate of substitution of $[Fe_4(SPh)_{10}]^{2-}$ is consistent with this proposal.

"All or Nothing" Reactivity. The mechanisms proposed in this paper rationalize the previously reported "all or nothing" behavior.[5] Studies on the reaction of $[Fe_4(SPh)_{10}]^{2-}$ with sulfur to form $[Fe_4S_4(SPh)_4]^{2-}$ in MeCN occur according to the stoichiometry shown in eq 9 and an "all or nothing" reactivity. Thus, by using a stoichiometric excess of $[Fe_4(SPh)_{10}]^{2-}$, sulfur reacts completely with one tetranuclear cluster before starting reaction with another. We have now shown that this behavior is general for this type of cluster. Thus, the ^1H NMR spectrum of the reaction mixture formed by mixing $[M_4(SPh)_{10}]^{2-}$ (M = Fe or Co) with 3 mol equiv of PhS^- showed that about half of the cluster remained unreacted, consistent with the stoichiometry of eq 10. Analogous experiments with $[MoS_4]^{2-}$ are not so clear-cut but indicate similar behavior. A complicating feature in quantifying the product distribution in the reactions with $[MoS_4]^{2-}$ is the competitive formation of $[M(SPh)_4]^{2-}$.

$$[Fe_4(SPh)_{10}]^{2-} + n\text{S} \rightarrow (n/4)[Fe_4S_4(SPh)_4]^{2-} + ((4-n)/4)[Fe_4(SPh)_{10}]^{2-} + (3n/4)\text{RSSR} \quad (9)$$

$$[M_4(SPh)_{10}]^{2-} + n\text{PhS}^- \rightarrow (2n/3)[M(SPh)_4]^{2-} + ((6-n)/6)[M_4(SPh)_{10}]^{2-} \quad (10)$$

$$[M_4(SPh)_{10}]^{2-} + n[MoS_4]^{2-} \rightarrow n[S_2MoS_2M(SPh)_2]^{2-} + ((4-n)/4)[M_4(SPh)_{10}]^{2-} + (n/2)\text{PhS}^- \quad (11)$$

Summary

Herein, we have reported kinetic studies on the reactions of the "adamantane-shaped" clusters $[M_4(SPh)_{10}]^{2-}$ (M = Fe or Co) with $[MoS_4]^{2-}$ or PhS^-. The reactions ultimately result in the complete rupture of the cluster but are initiated by substitution reactions. Both associative (with PhS^-) and dissociative (with $[MoS_4]^{2-}$) substitution mechanisms operate. However, the key step in the rupture of the cluster is the cleavage of μ-SPh linkages. Such cleavage is a natural consequence of an associative pathway if the metal site is to retain four-coordination. It is the cleavage of μ-SPh which opens up a vacant site on another M site so that a further nucleophile can bind. Thus, the reactivity of the adjacent M site is initiated by the first substitution reaction. The connectivity between all four M sites and the cleavage of interconnecting μ-SPh linkages means that, after the initial substitution step, reactions at all the other M sites rapidly ensue, resulting in the "all or nothing" reactivity of $[M_4(SPh)_{10}]^{2-}$.

The results presented herein allow us to compare the relative rates of substitution of the Fe and Co sites in the two structurally analogous clusters. For both the dissociative ($k_3^{Co}/k_3^{Fe} = 7.4$) and associative ($k_1^{Co}/k_1^{Fe} = 2.6$) pathways, the Co cluster is more labile. It seems likely that this is due to the cleavage of the leaving group being a dominant factor in both pathways.

Finally, it is worth commenting on the involvment of $[Fe_4(SPh)_{10}]^{2-}$ as an intermediate in the synthesis of heteronuclear Fe−S-based clusters containing $\{MFe_3S_4\}^{n+}$ cuboidal cores. The initial step in the construction of the cluster involves the disruption of the adamantane structure and formation of both binuclear and linear trinuclear species such as $[S_2MS_2Fe(SPh)_2]^{2-}$ and $[(PhS)_2FeS_2MS_2Fe(SPh)_2]^{n-}$. There is no direct pathway for the formation of a tetranuclear cuboidal cluster from a tetranuclear adamantane cluster. It seems likely that the same is true for the reaction with sulfur to form $[Fe_4S_4(SPh)_4]^{2-}$.

(20) Izutsu, K. *Acid−Base Dissociation Constants in Dipolar Aprotic Solvents*; Blackwell-Scientific: Oxford, 1990; p 17.
(21) Henderson, R. A.; Oglieve, K. E. *J. Chem. Soc., Dalton Trans.* **1993**, 1467.
(22) Henderson, R. A.; Oglieve, K. E. *J. Chem. Soc., Dalton Trans.* **1993**, 1473.
(23) Henderson, R. A.; Oglieve, K. E. *J. Chem. Soc., Chem. Commun.* **1994**, 377.
(24) Gronberg, K. L. C.; Henderson, R. A.; Oglieve, K. E. *J. Chem. Soc., Dalton Trans.* **1997**, 1507.
(25) Almeida, V. R.; Gormal, C. A.; Gronberg, K. L. C.; Henderson, R. A.; Oglieve, K. E.; Smith, B. E. *Inorg. Chim. Acta* **1999**, *291*, 212.

Acknowledgment. We thank John Innes Foundation for a studentship (to Z.C.), Shirley Fairhurst for assistance with the NMR spectroscopy, and Kay E. Oglieve for contributions in the early stages of this research.

Supporting Information Available: Tables of kinetic data. This material is available free of charge via the Internet at http://pubs.acs.org.

IC020284J